Jpn J Clin Oncol 2006;36(2)85–92
doi:10.1093/jjco/hyi227

Chromosomal Numerical Abnormality Profiles of Gastrointestinal Stromal Tumors

Kimihiro Yamashita[1,2], Hisaki Igarashi[1], Yasuhiko Kitayama[1,3], Takachika Ozawa[4], Shinichiro Kiyose[5], Hiroyuki Konno[6], Teruhisa Kazui[2], Shumpei Ishikawa[7], Hiroyuki Aburatani[7], Fumihiko Tanioka[1,8], Masaya Suzuki[1,9] and Haruhiko Sugimura[1]

[1]Department of Pathology and [2]Department of Surgery, Hamamatsu University School of Medicine, Hamamatsu, Shizuoka, [3]Department of Pathology, Shizuoka Saiseikai General Hospital, Shizuoka, [4]Department of Pathology, Hamamatsu Medical Center, Hamamatsu, Shizuoka, [5]JOKO Corporation, Hongo, Bunkyo-ku, Tokyo, [6]Department of Digestive Surgery, Hamamatsu University School of Medicine, Hamamatsu, Shizuoka, [7]Department of Genome Science, RCAST, Tokyo, [8]Department of Pathology and Laboratory Medicine, Iwata City Hospital, Iwata, Shizuoka and [9]Information System Division, Biosafety Research Center, Foods, Drugs, and Pesticides, Iwata, Shizuoka, Japan

Received June 17, 2005; accepted December 1, 2005; published online February 1, 2006

Background: Biological variations in and the heterogeneity of gastrointestinal stromal tumors (GISTs) are well known, but chromosomal numerical abnormality (CNA) has not been fully examined especially in this context. The aim of this study is to test CNA as a possible biological predictor of biological behavior of GISTs.
Method: We applied microwave-assisted FISH protocol to pathological archives of GIST tumors displaying different clinical features to characterize the CNA profile of these tumors. A panel of 18 centromere enumeration probes (CEP) and 24 bacterial artificial chromosome (BAC) or P1-derived artificial chromosome (PAC) probes containing genes like Aurora kinases (AURKs) and other candidate genes involved in human carcinogenesis were used. CNA profiles, histopathological risk categorization and Ki-67 labeling indexes of 23 primary and/or metastatic GIST tumors of 12 subjects (both primary and metastatic in 7 subjects) were compared between primary GIST with and without metastases, and between metastatic and primary portions in 7 individuals.
Results: CNA in the primary sites was more extensive in the GISTs with recurrence and metastasis than in those without, especially as to the loss of chromosome 20 and genomic imbalance of *AURKA*-containing BAC probe on 20q in the cases with metastasis. The consistent loss of one allele of chromosome 14q was also noted. Interestingly, both primary and metastatic tumors in identical individuals had similar CNA profiles.
Conclusion: The extent of CNA differed between GISTS with and without recurrence or metastasis; thus, FISH analysis of specimens from the primary sites may predict the biological behavior of this tumor.

Key words: chromosomal numerical abnormality – chromosomal instability – GIST – FISH – microwave

INTRODUCTION

Gastrointestinal stromal tumors (GISTs) are recently characterized mesenchymal tumors of the gastrointestinal tract that arises not from the tissues of gastrointestinal epithelium but from the connective tissue of the gastrointestinal wall. Its biological behavior varies from slow and limited expansive growth (low grade) to very proliferative and metastatic one (high grade). The molecular definition of this tumor has been established as a gain-of-functional mutation of *KIT*, leading to its overexpression in tumors (1). Currently, predictions of the biological behavior of GISTs mainly depend on the clinicopathological phenotype, such as the presence of hematogeneous metastasis, the extent of dissemination, tumor size and mitotic index. However, it is sometimes difficult to develop plan for the treatment of this tumor at the time of diagnosis or resection based only on the currently available markers.

In this report, we surveyed the numerical chromosomal aberrations of most of the chromosome centromeres found in this tumor. Additionally, alterations of several loci, such

For reprints and all correspondence: Haruhiko Sugimura, Department of Pathology, Hamamatsu University School of Medicine, 1-20-1, Handayama, Hamamatsu, Shizuoka 431-3192, Japan. E-mail: hsugimur@hama-med.ac.jp

as those for Aurora kinases, that are amplified in substantial portion of human malignant tumors (2–5), were tested. We also visualize the changes at these loci, whereas previous comparative genomic hybridization (CGH) studies only disclosed the loss of the loci.

MATERIALS AND METHODS

Subjects and Clinicopathological Assessments

Tissue microarrays containing 23 GIST tumors from 12 patients were constructed by tissue microarrayer using KIN-1 (Azumaya Corporation, Tokyo, Japan). These tumor specimens consisted of 11 primary and 12 metastatic tumors, 7 cases having had both primary and metastaic tumors. The clinical profiles are summarized in Table 1. The subjects consisted of five men and seven women, with a mean age at the time of first diagnosis of 58.7 ± 17.0 years. Twenty-three tumor specimens were available for the analysis. The primary sites were the stomach in seven cases, the small intestine in two and the omentum/mesenterium in three. Overall, eight cases showed metastasis or recurrence: four metastases to the liver, one metastasis to the small intestine, and four cases of recurrence and peritoneal dissemination. The histological features of the primary sites were spindle-type in five, epithelioid-type in five, mixed-type in one and unrecorded in one. The primary site tumor of these patients were categorized into a high- and a low-risk group based on the currently used criteria (6), i.e. the cases were estimated based on the follow-up information of any recurrence or other malignant behaviors in addition to histopathological features (sizes and mitotic counts). All the cases were closely surveyed for up to 14 years after diagnosis. Two pathologists independently evaluated the morphological features of these cases. The mitotic index was calculated in each case by summing the number of mitotic figures in 50 high power fields (20× objective). Thus, seven cases were obviously

Table 1. Summary of clincopathologic features in 23 GISTs

Case	Gender	Age	Clinical status	Tumor origin	Recurrence period	Maximum tumor size (cm)	Mitotic count (/50HPF*)	Morphology	Malignant potential**
1	Male	43	Primary	Mesenterium		13	10	Mixed	High risk
			Liver metastasis		Synchronous	7	12	Mixed	High risk
			Intestinal metastasis		Synchronous	Unspecified	12	Mixed	High risk
2	Female	63	Primary	Stomach		3.8	1	Epithelioid	Low risk
			Liver metastasis		4 year	2.6	6	Epithelioid	Intermediate
3	Male	49	Primary	Omentum		>10	0	Spindle	High risk
			Liver metastasis		14 year	17	14	Epithelioid	High risk
4	Male	49	Primary not available	Stomach			Unknown details		
			Liver metastasis		4 year	2.7	3	Mixed	Low risk
			Recurrence			1.8	6	Mixed	Intermediate
5	Female	74	Primary	Stomach		20	1	Epithelioid	High risk
			Liver metastasis		Synchronous	2.6	3	Epithelioid	Low risk
			Peritoneal dissemination		Synchronous	2 (multiple)	7	Epithelioid	undefined
6	Male	72	Primary	Stomach		4	9	Spindle	High risk
			Recurrence		3 year	1	20	Spindle	High risk
7	Male	75	Primary	Stomach		18	11	Epithelioid	High risk
			Recurrence		1 year		23	Epithelioid	High risk
			Re-recurrence		1 year		50	Epithelioid	High risk
8	Female	55	Primary	Small intestine		6	1	Epithelioid	Intermediate
			Recurrence		3 year	2 (multiple)	3	Epithelioid	Low risk
					follow-up (absence of recurrence)				
9	Female	75	Primary	Stomach	3 year	2	3	Spindle	Low risk
10	Female	80	Primary	Stomach	2 year	8	6	Spindle	High risk
11	Female	53	Primary	Omentum	4 year	15	8	Epithelioid	High risk
12	Female	19	Primary	Small intestine	3 year	15	2	Spindle	High risk

*HPF, high power field.
**Malignant potential classification according to the article of Fletcher [reference (6)]. GISTs were classified 'very low risk', 'low risk', 'intermediate risk' and 'high risk' based on tumor size and the mitotic index.

high-grade malignant GISTs, because these patients had intraperitoneal recurrences or hematogenous metastases to the liver. However, four cases appeared to be low-grade GISTs. This study has been approved by Institutional Review Board of Hamamatsu University School of Medicine (12-11).

c-Kit Immunostaining

Samples on the slides were rinsed in xylene–alcohol dewaxing series. The slides were boiled in Target Retrieval solution (DakoCytomation, Glostrup, Denmark) as a pretreatment. Endogenous peroxidase was blocked with 0.3% hydrogen peroxide/ethanol. Following incubation with the c-Kit (CD117) rabbit polyclonal anti-human antibody (DakoCytomation), specimens were incubated with peroxidase-labeled-dextran polymer-reagent-conjugated goat anti-mouse immunoglobulin antibody (Chemomate; DakoCytomation). All the cases were strongly positive for cytoplasmic KIT expression.

Ki-67 Labeling Index

The Ki-67 labeling index was determined in all the tumors. Ki-67 immunostaining was performed according to a previously described procedure. Briefly, sections were subjected to autoclave-antigen retrieval in citric acid buffer at pH 6.0 for 15 min at 121°C. Endogenous peroxidase was blocked with 0.3% H_2O_2 in methanol for 15 min. After washing in phosphate-buffered saline (PBS), the sections were incubated with the primary antibody (MIB-1; DakoCytomation) for 60 min at room temperature. After another wash in PBS, the sections were incubated with the secondary antibody and Simple Stain MAX-PO (M) (Nichirei, Tokyo, Japan) for 30 min at room temperature. The sections were counterstained with hematoxylin. The nuclei with distinctly brown nuclear immunoreactivity for Ki-67 were counted. The Ki-67 labeling index was calculated using the percentage of MIB-1-positive cell among 500 cells.

FISH Probes

Commercially available locus-specific identifier (LSI) probes, HER2/neu and p53/17p13.1, were used according to the manufacturer's instructions (Vysis, Downers Grove, IL, USA). Self-made chromosome-specific probes were made from bacterial artificial chromosome (BAC) or P1-derived artificial chromosome (PAC) DNA containing the following symbol genes (gene name representing the clone in parentheses): RP5-1167H4 (*AURKA*) on 20q, RP11-849F2 (*AURKB*) on 17p, RP11-12C9 (*AURKC*) on 19q, RP3-394P21(*PAX7*) on 1p, RP11-82P18(*LRP1B*) on 2q, RP11-128C13(*PDGFR*) on 5q, RP11-149I2(*p15*) on 9q, RP11-174I10(*RB1*) on 13q, RP5-857M17(*ID1*) and RP1-1J6(*TOP1*) on 20q, and RP1-76B10(*NF2*) on 22q. For the long arm of chromosome 14, where a high frequency of deletions has been reported for GISTs, four probes from RP11-356O9, RP11-293M10, RP11-589M4 and RP11-815P21 were used. BAC probes at the near-centrometric lesions of chromosomes 5 (RP11-91I22), 13 (RP11-61K9), 14 (RP11-516D7), 19 (RP11-206O6) and 22 (RP11-66F9) were also used (Advanced Geno Techs Co., Tsukuba, Japan). Purified BAC or PAC DNA was labeled with spectrum orange or green using a nick translation kit (Vysis). A panel of alpha-satellite DNA probes, Centromere Enumeration Probes (CEPs; Vysis) identifying numbers of chromosomes 1–4, 6–12, 15–18, 20, X and Y was applied to detect chromosomal numerical abnormalities. A CNA profile was defined as the sum of histograms of each CEP signal in each tumor cell based on up to 100 tumor cells, as shown in the previous report (10). CEP signals were used as a reference for locus-specific probes on the arms of the corresponding chromosomes. All the probes were detected two signals in each normal cell, when the cells' maximum diameters were visible in the paraffin sections [data not shown, refer to (7)].

The probes used in this study are listed in the supplementary table with counting method (available at http://www.jjco.oxfordjournals.org).

Microwave-assisted FISH

The microwave (MW)-assisted FISH protocol was described elsewhere (8). Sections were deparaffinized with three successive, 5 min rinses in xylene followed by five washes in ethanol and MW heating for 10 min in a 0.01 M citrate buffer (pH 6.0). After treatment in 0.3% pepsin/0.01 N HCl for 10 min at 37°C, the samples were aged (to improve membrane permeability) in 0.1% NP-40/2× SSC for 30 min at 37°C and their DNA was denatured by treatment in 70% formamide/2× SCC for 5 min at 85°C. Ten microliters of the probe solution (hybridization buffer, 7 μl; CEP probes, 1 μl; LSI, BAC or PAC probe, 1 or 2 μl; distilled water, 1 or 0 μl) was then placed on a glass slide and covered with a cover slip. The sample slides with the hybridization mixture were then put in a microwave processor (MI-77; Azumaya Corporation). The samples were irradiated for 3 s at 2 s intervals (2.45 GHz, 300 W) with the temperature sensor set at 42°C. Each specimen was subjected to MW-intermittent irradiation during the initial 1 h of *in situ* hybridization and was then placed overnight in an incubator set at 37°C. DAPI I (4′,6-diamidino-2-phenylindole, 1000 ng/ml; Vysis) was used for the nuclear counterstaining. The samples were promptly observed using a fluorescence microscope (BX-51; Olympus, Japan) equipped with epi-fluorescence filters and a photometric CCD camera (Sensicam; PCO Company, Kelheim, Germany). The captured images were digitized and stored using an image analysis program (MetaMorph; Molecular Devices, CA, USA). The number of signals per cell was counted for a total of 100 or more cell nuclei.

Quantitative Image Analysis

In addition to manual counting, we also used the MetaMorph image analysis software to quantitate the signals in the tumor cell area. To acquire a stack image, the signals were filtered using a 'Top Hat' filter so that only signals greater than

the defined value were incorporated. Then, the number of signals in the area was automatically counted in at least five different fields for each sample. The percent ratio of LSI, BAC or PAC probes to the corresponding CEP or near-centromere probe signal was calculated. This method was used to analyze *AURKA*, *AURKB*, *AURKC*, *HER2* and p53. We did not automatically quantitate the signals from the 14q probes because a reference centromere probe was not available. Instead, we manually measured the 14q probe signal in that region.

Control Count

To monitor the reliability of our experimental protocol, tissues from normal control specimens (normal mucosa of the stomach and colon) were analyzed and the ratios and variations in the signals were obtained. In some of cases, automatic counting using MetaMorph was performed. For each probe, five control specimens of normal gastrointestinal mucosa were examined. The cut-off value was set at mean ± 3 SD of the signal number for autosomes.

Statistical Analysis

All the values were described as the mean ± SD. A Fisher's exact test and a Wilcoxon rank test were performed to compare the whole and particular chromosomal numerical features between metastatic and non-metastatic cases. Comparisons were made among CNAs of the primary sites. We also calculated CNAs of all the specimens we examined. Furthermore, we compared the CNAs of the primary sites and the available corresponding metastatic tumors (seven pairs). SAS ver. 9.1 (SAS Institute, Inc., Cary, NC, USA) was used, and a P-value <0.05 was considered statistically significant. All the statistical assessment was done by one of the authors (M.S.), a professional statistician.

RESULTS

The malignant potentials, according to Fletcher's classification, were high-risk in eight cases, intermediate-risk in one case and low-risk in two cases. One of the cases originally categorized as low-risk based on this criteria experienced a recurrence and metastasis during the follow-up period (Case 2). Both the Ki-67 labeling index and mitotic index of the metastatic or recurrent cases (seven primary tumors) were not significantly different from those of the non-metastatic cases (four primary tumors) (Table 2). The sizes of metastatic and non-metastatic cases were not different either.

Chromosomal Numerical Abnormality and Chromosome Arm-specific Examination of GISTs

Figure 1 is a representative graph showing the CNA profile of Case 1. The deviation in the numbers of each chromosome is shown as a dot in the graph. The mean and standard deviation of each chromosome when up to 100 cells were counted are indicated. The asterisks indicate chromosomes with values

Table 2. Mitotic count and Ki-67 labeling index between metastatic and non-metastatic cases

	With metastasis (n = 7)	Non-metastasis (n = 4)	
	mean ± SD	mean ± SD	P-value
Mitotic count	0.094 ± 0.100	0.095 ± 0.055	0.775
Ki-67 labeling index	1.0714 ± 1.5585	0.625 ± 0.4349	1.000

that surpassed the cut-off point. The cut-off point for the signal number was set for each CEP and LSI probe based on the mean ± 3 SD of the numbers obtained from the normal epithelial cells. Figure 2 showed representative images of CNA, loss of chromosome 6, 18, Y.

Generally, the CNA profiles, a general view of the changes of each chromosome as reported in the previous papers (6–10), of the GISTs were nearly diploid, with regard to numbers of centromeres. Gain and loss was defined as significant increase and decrease of numbers of signals compared with the reference, two for autosomes and female Xs and one for Y chromosome or male X in at least 100 tumor cells. To exclude the chance of artificial gains due to stratification of the cells and misdiagnostic loss due to incomplete section, non-tumor controls were calculated and the cut-off value of three times of standard deviations were defined.

When CNA in primary tumors was compared between metastatic and non-metastatic cases, the losses of the chromosomes such as CEP6 were found only in the primary tumor with metastasis (Table 3). The primary site tumors without metastasis did not lose any one of the alleles (Table 4). As to the changes in dosage of chromosome 20, there was no such change in the primary site tumors without metastases (data not shown). Interestingly, in seven pairs of primary and metastatic tumors, the CNA profiles using CEP probes were identical.

An amplification of chromosome 17 was found in only one case. However, the LSI probe, Her2 and p53 signals were not altered in any of the cases. Using other locus-specific BAC or PAC clones, we identified the consistent loss of 14q (RP11-356O9, RP11-589M4, RP11-293M10, RP11-815P21) (Fig. 3a). Especially, the RP11-293M10 containing *FOS* gene located in 14q24.3 was deleted in 18 out of 23 specimens (78.3%). The loss of 14q12-13 (RP11-356O9) was seen in 7 specimens (30.4%), 14q21.3 (RP11-589M4) was seen in 9 (39.1%) and the loss of 14q32 (RP11-815P21) was seen in 12 specimens (52.2%) (Fig. 3b and c). The loss of heterozygosity of 14q was seemed to occur more frequently among the cases with metastasis than the cases without metastasis, but no significant difference was detected between the two groups (Table 4).

LSI/CEP-relative Signal Numbers

Since the amplification of Aurora kinases has been reported for some malignancies, we quantified those loci using computer-determined assisted software in the 22 of 23 cases. A cut-off value (the range between safety margins; the values inside those could be obtained by errors) of 0.89–1.11 was

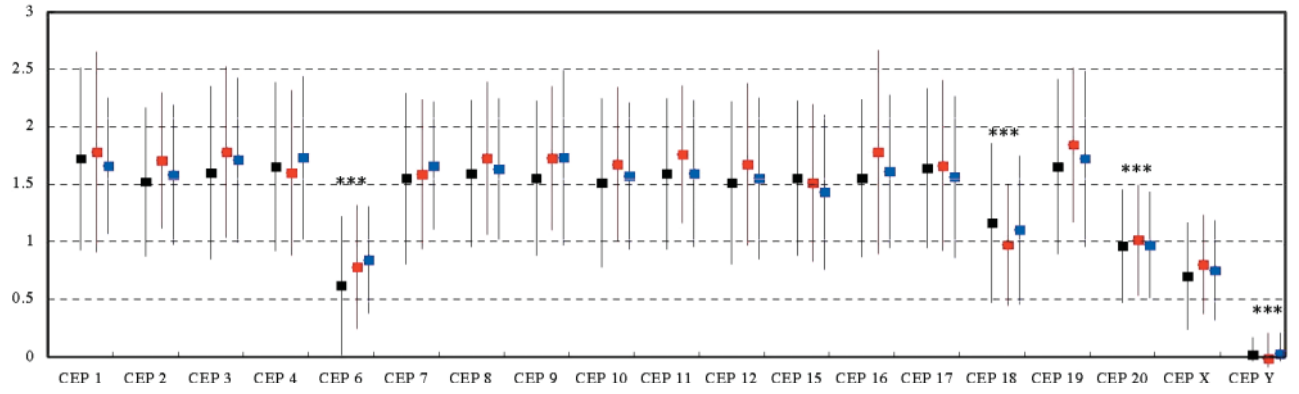

Figure 1. Ploidy and CNA in Case 1. For each CEP probe, the mean signal number per nuclei and the SD range is plotted along the *y*-axis. An asterisk (*) indicates a chromosome loss. The primary site and metastatic tumor had similar CNA profiles. Red, blue and black vertical lines represent liver metastasis, intestinal metastasis and primary site, respectively.

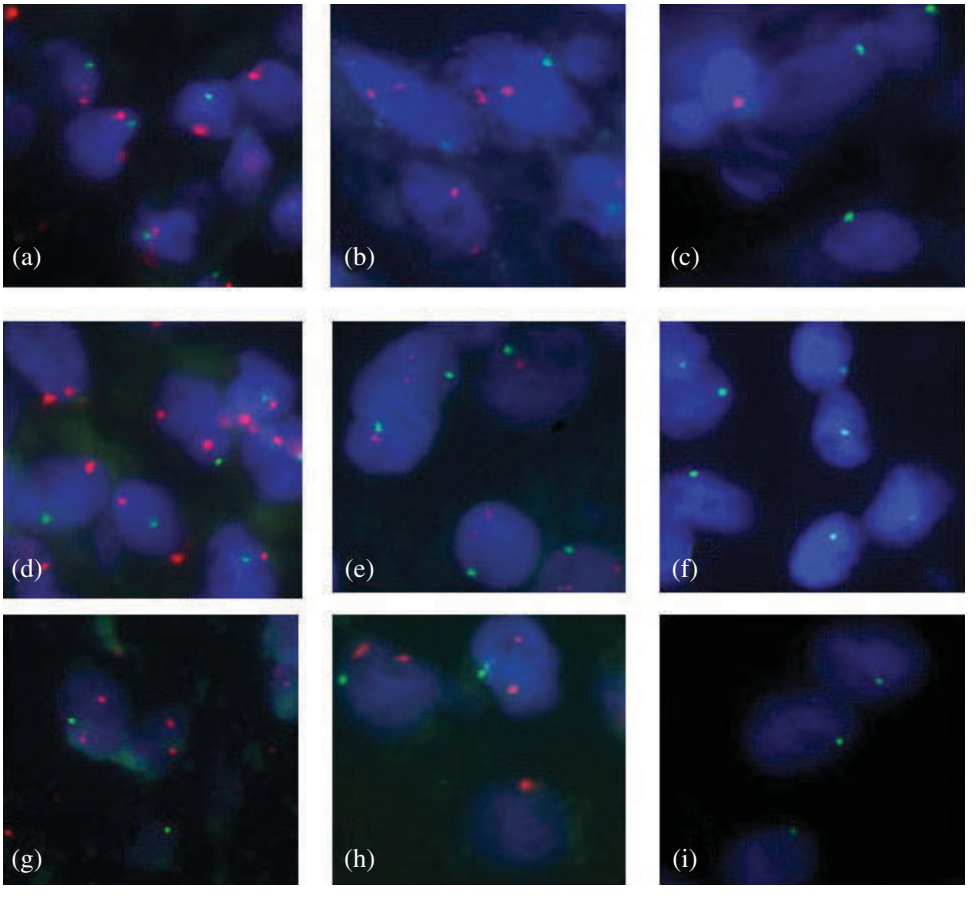

Figure 2. Representative images of chromosomal numerical FISH studies using centromeric alpha satellite probes (Vysis) in Case 1. (a), (b) and (c) are for the primary tumor; (d), (e) and (f) are for the liver metastasis; (g), (h) and (i) are for the intestinal metastasis. One CEP 6 (green) signal and two CEP 1 (red) signals in each nuclei (a, d and i), one CEP 18 (green) signal and two CEP 16 (red) signals (b, e and h) and no CEP Y (red) signal and one CEP X (green) signal (c, f and i) suggest the loss of chromosomes 6, 18 and Y, respectively.

determined by calculating the value for normal samples. The mean of five measurements of the RP5-1167H4/CEP20 ratio was larger than 1.00 in all the cases tested. In Case 1, automatic counting yielded elevated *AURKA*/CEP20 ratios (Fig. 4). The ratio in Case 1 was 1.99 for the primary tumor, 1.85 for the liver metastasis and 3.38 for the metastatic tumor in the small intestinal wall. In Case 2, automatic counting results were not available because of the specimens' conditions, and conventional counting yielded ratios of 2.02 and 1.83 for the primary and metastatic tumors, respectively. In Case 3, the primary tumors were not qualitatively available for FISH analysis and 1.46 for liver metastasis; a gain of *AURKA* was noticed

Table 3. Chromosomal numerical abnormality profiles of 23 GISTs

Clinical status	CNA
Case 1	
Primary	Loss: 6, 18, 20, Y
Liver metastasis	Loss: 6, 18, 20, Y
Intestinal metastasis	Loss: 6, 18, 20, Y
Case 2	
Primary	Loss:10, 20
Liver metastasis	Loss: 4, 10, 20, X
Case 3	
Primary	NA*
Liver metastasis	Loss: 2, gain: 8
Case 4	
Primary not available	
Liver metastasis	Loss: 4, 16, gain: 17
Recurrence	Loss: 16, gain: 17
Case 5	
Primary	Loss: 10, 16
Liver metastasis peritoneal dissemination	Loss: 10, 16
Case 6	
Primary	Loss: 6
Recurrence	Loss: 6
Case 7	
Primary	Loss: 18
Recurrence	Loss: 18
Re-recurrence	Loss: 18
Case 8	
Primary	Loss: 15
Recurrence	Loss: 15
Case 9	
Primary	Normoploidy
Case 10	
Primary	Normoploidy
Case 11	
Primary	Normoploidy
Case 12	
Primary	Normoploidy

*NA, not available.
CNA, chromosomal numerical abnormality.

in this specimen. In all the other cases, *AURKA*/CEP20 were within the cut-off value. In summary, a relative gain of gene dosage in the *AURKA* locus only occurred in cases with liver metastases (three out of four cases versus none of the other nine cases). No significant loss or gain of *AURKB* (RP11-849F2), *AURKC* (RP11-12C9) or other locus-specific probes (Her2, p53) was observed in the tumors (data not shown).

Table 4. Numbers of chromosomes numerically abnormality of metastatic and non-metastatic cases

		Total numbers of CEP	Number of CNA	*P*-Value
Loss	Metastasis ($n = 6$)	126	11	0.003
	Non-metastasis ($n = 4$)	90	0	

CEP, centromere enumeration probe; CNA, chromosomal numerical abnormality.

DISCUSSION

Although there have been several criteria frequently used for predicting the biological behavior of GIST tumors, clinical outcomes remains difficult to predict based on an ordinary pathological examination alone. For example, in our own series, one of the patient indeed developed a metastasis even though the traditional index had classified the patient's tumor as low-risk. Furthermore, tumor size, mitotic indexes and the Ki-67 labeling index of the primary tumors in our series were not related to the recurrence of GIST, unlike the findings of previous reports.

Only one group other than ourselves seems to have systematically investigated chromosomal changes in GISTs. Debiec-Rychter et al. (11) used FISH to visualize chromosomal numerical aberrations and 14q, 22q, 1p and 13q loss in their 23 cases. They reported that multiple chromosomal abnormalities appeared even in the 'early' stage of GIST pathogenesis (their criteria for malignant GIST depended only on the mitotic count) and they stressed the importance of the early loss of specific tumor suppressor genes in GIST. Interestingly, their data can be interpreted as showing chromosomal loss, rather than gain, in GISTs, which is consistent with the result of our study.

We have applied our method of MW-assisted FISH to common tumors such as gastric and breast cancers (7–10). The result described here for GIST together with that of the other group contrasts that seen for stomach and breast cancers, which exhibit extensive, aneuploidal changes (7–10).

As we previously noted (10), CNA profile is sometimes useful for identifying the lineage of tumors and tracing tumor clones. Importantly, even though no particular chromosome was responsible for the metastatic potential, the grade of CNA was greater in cases of tumors with metastasis. As to lineage, the CNA profiles were mostly identical for the primary and the metastatic sites, similar to the result of a previous study on p53 in the colorectal metastatic process (12). Thus, CNA in the primary GIST may be a persistent characteristic of GIST during metastasis and may be a predictive marker for metastasis or recurrence.

The quantification of FISH signals sometimes requires tedious manual counting. We applied an automatic counting procedure for convenience. This system does not include confocal microscope; thus, we carefully set the cut-off value so that misdiagnosis due to incomplete view of the cells could be

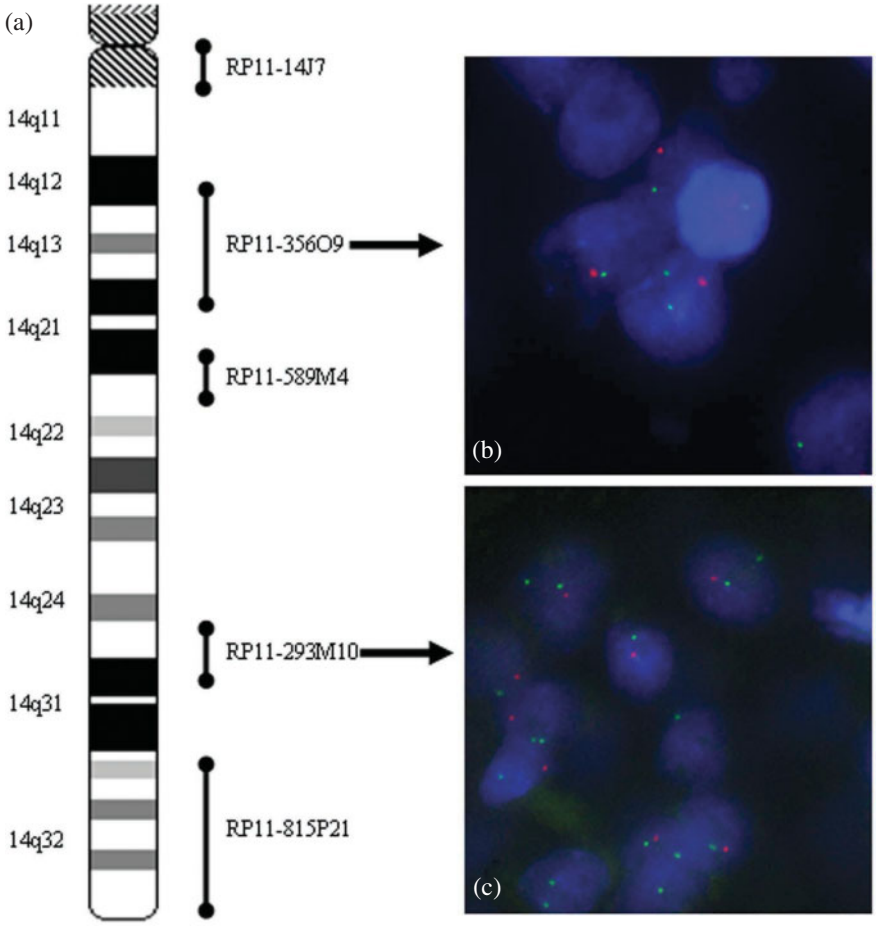

Figure 3. (a) Ideogram of chromosome 14's long arm showing the locations of BAC, RP11-14J7 (14q11), RP11-356O9 (14q12-13), RP11-589M4 (14q21.1), RP11-293M10 and RP11-815P21 probes. Representative 14q locus BAC DNA probes, RP11-356O9 (b) and RP11-293M10 (c), labeled with spectrum orange and the near centromeric probe, RP11-14J7 (14q11.1), labeled with spectrum green were used. One orange signal and two green signals per nuclei indicate the deletion of these loci.

Table 5. Alterations of the specific loci in metastatic and non-metastatic case

	Numbers of tumors with changes (%)	
Chromosome locus with loss	Tumor with metastasis (n = 7)	Tumor without metastasis (n = 4)
14q12-q13	3 (43)	0 (0)
14q21.3	3 (43)	1 (25)
14q24.3	6 (86)	3 (75)
14q32	5 (71)	2 (50)
20q11	1 (14)	0 (0)
20q12-q13	2 (29)	0 (0)
20q13.2	2 (29)	0 (0)

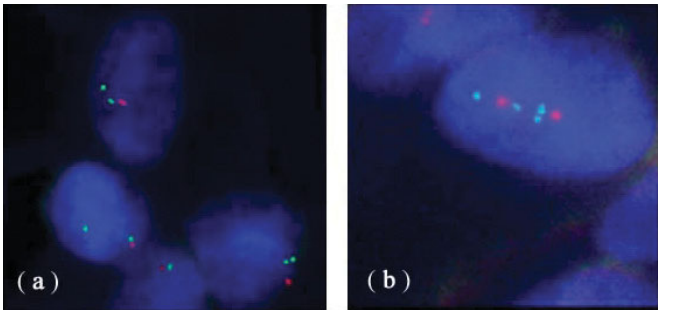

Figure 4. Representative FISH images used in the automatic analysis. The image shows double-color FISH using *AURKA*, the PAC clone DNA probe labeled with spectrum green, and centromeric alpha satellite probe of chromosome 20 (CEP20) labeled with spectrum orange (Vysis). (a) One CEP20 signal and two *AURKA* signals indicate the loss of chromosome 20 and relative gain of *AURKA* gene in Case 2. The *AURKA*/CEP20 mean relative ratio was 1.99. (b) *AURKA* relative gain in Case 3. The mean relative ratio was 1.31.

minimized. The method adopted in this paper consisted of an automatic counting procedure using computer software MetaMorph (Molecular Devices), and it enabled us to quickly and objectively count the FISH signals. Calculating the ratio of the two signals provided a better resolution of relative gain in *AURKA* versus centromere 20 and was consistent with the result of manual counting; thus, this procedure can alleviate the work load of molecular diagnostic facilities. Furthermore, this application could enable relative chromosomal alterations in any locus to be estimated objectively when using LSI probe.

Relative increase in dosage of *AURKA* locus seems to be a specific change found in metastatic GISTs, implying that *AURKA* was associated with hematogenous metastasis in GISTs. The values of 1.83 and 1.46 may reflect the heterogeneity of the tumors.

Specific and consistent loci loss in GISTs has been proposed. We verified and visualized these changes using archived tissues. As shown in the Table 4, our results regarding deletions are generally consistent with those published by Debiec-Rychter et al. (13). The 14q deletions were the most common chromosomal alteration among our cases, but the frequency of this alteration was similar for primary tumors with metastasis and primary tumors without metastasis; thus, these deletions probably do not affect the biological behavior of GISTs. Alterations of 1p, 13p and 22p (14–17) described in previous CGH studies were not detected in the present study, but considerable changes in 13q and 22q were noted. We also detected the changes in 9q and 10q in one case, as shown by a genome-wide allele dosage analysis using an SNP microarray (data not shown).

In conclusion, non-random changes in chromosomes were visualized among the pathology archived GISTs specimens. In particular, we successfully identified a 20q gain, especially in metastatic cases by MW-assisted FISH. This finding must be confirmed in a larger number of cases before it can be used as a practical predictor. MW-assisted FISH may be a helpful additional laboratory procedure for predicting the biological behaviors of GISTs, metastasis or recurrence.

Acknowledgments

This work was supported in part by a Grant-in-Aid from the Ministry of Health, Labour and Welfare for the 2nd-term Comprehensive 10-Year Strategy for Cancer Control, from the Smoking Research Foundation, and from the Ministry of Education, Culture, Sports, Science and Technology of Japan for Scientific Research (15290125) on Priority Area (17015017) and the 21st century COE program 'Medical Photonics' (Hamamatsu University School of Medicine), and by a Grant-in-Aid from the Foundation for Promotion of Cancer Research (2003).

References

1. Miettinen M, Sobin LH, Lasota J. Gastrointestinal stromal tumors of the stomach: a clinicopathologic, immunohistochemical, and molecular genetic study of 1765 cases with long-term follow-up. *Am J Surg Pathol* 2005;29:52–68.
2. Jeng YM, Peng SY, Lin CY, Hsu HC. Overexpression and amplification of Aurora-A in hepatocellular carcinoma. *Clin Cancer Res* 2004;10: 2065–71.
3. Li D, Zhu J, Firozi PF, Abbruzzese JL, Evans DB, Cleary K, et al. Overexpression of oncogenic STK15/BTAK/Aurora A kinase in human pancreatic cancer. *Clin Cancer Res* 2003;9:991–7.
4. Sakakura C, Hagiwara A, Yasuoka R, Fujita Y, Nakanishi M, Masuda K, et al. Tumour-amplified kinase BTAK is amplified and overexpressed in gastric cancers with possible involvement in aneuploid formation. *Br J Cancer* 2001;84:824–31.
5. Tanaka T, Kimura M, Matsunaga K, Fukada D, Mori H, Okano Y. Centrosomal kinase AIK1 is overexpressed in invasive ductal carcinoma of the breast. *Cancer Res* 1999;59:2041–4.
6. Fletcher CD, Berman JJ, Corless C, Gorstein F, Lasota J, Longley BJ, et al. Diagnosis of gastrointestinal stromal tumors: a consensus approach. *Hum Pathol* 2002;33:459–65.
7. Kobayashi K, Kitayama Y, Igarashi H, Yoshino G, Kobayashi T, Kazui T, et al. Intratumor heterogeneity of centromere numerical abnormality in multiple primary gastric cancers: application of fluorescence *in situ* hybridization with intermittent microwave irradiation on paraffin-embedded tissue. *Jpn J Cancer Res* 2000;91: 1134–41.
8. Kitayama Y, Igarashi H, Sugimura H. Different vulnerability among chromosomes to numerical instability in gastric carcinogenesis: stage-dependent analysis by FISH with the use of microwave irradiation. *Clin Cancer Res* 2000;6:3139–46.
9. Kitayama Y, Igarashi H, Watanabe F, Maruyama Y, Kanamori M, Sugimura H. Nonrandom chromosomal numerical abnormality predicting prognosis of gastric cancer: a retrospective study of 51 cases using pathology archives. *Lab Invest* 2003;83:1311–20.
10. Nakamura R, Song JP, Isogaki J, Kitayama Y, Sugimura H. Multiple (multicentric and multifocal) cancers in the ipsilateral breast with different histologies: profiles of chromosomal numerical abnormality. *Jpn J Clin Oncol* 2003;33:463–9.
11. Debiec-Rychter M, Lasota J, Sarlomo-Rikala M, Kordek R, Miettinen M. Chromosomal aberrations in malignant gastrointestinal stromal tumors: correlation with c-KIT gene mutation. *Cancer Genet Cytogenet* 2001;128:24–30.
12. Maruyama K, Tanaka T, Baba S, Nakamura S, Endo Y, Sugimura H. p53 accumulation in colorectal cancer with hepatic metastasis. *Jpn J Cancer Res* 1996;87:368–76.
13. Debiec-Rychter M, Sciot R, Pauwels P, Schoenmakers E, Dal Cin P, Hagemeijer A. Molecular cytogenetic definition of three distinct chromosome arm 14q deletion intervals in gastrointestinal stromal tumors. *Genes Chromosomes Cancer* 2001;32:26–32.
14. el-Rifai W, Sarlomo-Rikala M, Andersson LC, Miettinen M, Knuutila S. DNA copy number changes in gastrointestinal stromal tumors—a distinct genetic entity. *Ann Chir Gynaecol* 1998;87:287–90.
15. Gunawan B, Bergmann F, Hoer J, Langer C, Schumpelick V, Becker H, et al. Biological and clinical significance of cytogenetic abnormalities in low-risk and high-risk gastrointestinal stromal tumors. *Hum Pathol* 2002;33:316–21.
16. Chen Y, Tzeng CC, Liou CP, Chang MY, Li CF, Lin CN. Biological significance of chromosomal imbalance aberrations in gastrointestinal stromal tumors. *J Biomed Sci* 2004;11:65–71.
17. Derre J, Lagace R, Terrier P, Sastre X, Aurias A. Consistent DNA losses on the short arm of chromosome 1 in a series of malignant gastrointestinal stromal tumors. *Cancer Genet Cytogenet* 2001;127:30–3.